Three to six ambiguities in immittance spectroscopy data fitting

2012 J. Phys.: Condens. Matter 24 175004

(http://iopscience.iop.org/0953-8984/24/17/175004)

IOP PUBLISHING JOURNAL OF PHYSICS: CONDENSED MATTER
J. Phys.: Condens. Matter **24** (2012) 175004 (11pp) doi:10.1088/0953-8984/24/17/175004

Three to six ambiguities in immittance spectroscopy data fitting

J Ross Macdonald

Department of Physics and Astronomy, University of North Carolina, Chapel Hill, NC 27599, USA

E-mail: macd@email.unc.edu

Received 24 January 2012, in final form 4 March 2012
Published 5 April 2012
Online at stacks.iop.org/JPhysCM/24/175004

Abstract
Several important ambiguities in immittance spectroscopy (IS) model data-fitting results are identified and illustrated by means of complex-nonlinear-least-squares (CNLS) fits of experimental and synthetic frequency response data. A well-known intrinsic ambiguity, following from Maxwell's electromagnetic equations, arises from the indistinguishability in external measurements of conduction and displacement currents. Usual fit models for either dielectric or conductive-system situations, such as the Davidson–Cole one, only involve a strength parameter, a dielectric constant, a characteristic relaxation time, and a fractional exponent and lead to no additional ambiguities. But the situation is different for more powerful and useful general models, such as ordinary or anomalous diffusion Poisson–Nernst–Planck ones: PNP and PNPA, used here, whose historical background, current status, and applicability are described and discussed herein. They apply to two different kinds of experimental IS situations and involve several additional, potentially free fit parameters, such as the mobilities of positive and negative charge carriers, and generation–recombination parameters that determine the partial or complete dissociation of a neutral entity of concentration N_0 into positive and negative charge carriers of equal concentration, c_0. Then, several additional ambiguities appear that may require information about the material system involved for their adequate resolution.

(Some figures may appear in colour only in the online journal)

1. Introduction

A primary problem in analyzing immittance spectroscopy (IS) data (or any data) is identifying a physically significant fitting model. Although it is frequently possible to show that a composite model including many free parameters, such as one, two, or even more Havriliak–Negami models (see [1] and section 2 herein) in series, parallel, or series–parallel, can lead to good or excellent frequency- and temporal-domain fits of experimental data, such empirical models are worthwhile only to represent data, not to allow identification and interpretation of the physico-chemical parameters and processes involved. In an ideal, non-chaotic world one might expect that it would be possible, given a set of good IS data, to find an unambiguous, meaningful model that best fitted the data with a minimum of free, physically significant parameters. But the real world is nearly infinitely various and perhaps no part of it can be fully represented by an ideal model, even though such models are essential to add to our understanding. Although Feynman rightly said 'Experiment is the sole judge of scientific truth', one should also consider Bohr's statement, 'Science is not a means of obtaining absolute truth. The real test of a scientific theory is not whether it is 'true' but whether it works'. Here we consider models that work.

Nevertheless, it should not be surprising that significant ambiguities may arise from data fitting in the IS domain. Here we describe some ambiguities in model selection and parameter interpretation even for physically realistic models. The results are interesting in themselves but, more importantly, they are valuable in suggesting what additional experimental information might be needed to allow resolution of the ambiguities by choosing the physically most appropriate of two virtually identical fits of the same data set: ones involving either two different fitting models or one model with two types of fit involving some different free parameter estimates.

An endemic ambiguity, potentially present for all IS models, is inherent in the impossibility of characterizing externally measured currents as being of either displacement or conduction type. This ambiguity, designated #1 here, was perhaps first illustrated and discussed in detail in the context of IS data fitting in 1999 [2]. It follows that even for completely blocking electrodes a conduction model (one involving mobile charges) in parallel with a dielectric constant can, in principle, lead to exactly the same response as a dielectric model (involving only dipoles and possibly higher multipoles) in parallel with a non-zero resistivity if required. In practice, however, one should not expect to find both a specific conductive model and a specific dielectric one that lead to exact agreement but, as demonstrated in [3][1] and herein, the agreement may be excellent and close enough to that arising only from the presence of small random errors in the data so that the ambiguity is confirmed for all practical purposes. Clearly, resolution of ambiguity #1, when possible, requires knowledge of additional information about the material involved and the experimental situation.

The remaining ambiguities discussed herein are only present, and not necessarily directly apparent, for conductive-system response models that can lead to estimates of more relevant parameter values than the ones generally used previously for the analysis of impedance spectroscopy data (e.g., [1, 4–22][2,3], roughly ordered by type of model). Most ones, such as the empirical Havriliak–Negami one, used for either dielectric or conductive data, involve a strength parameter, a characteristic relaxation time, and possibly one or two fractional power-law exponents. For conductive systems, the strength parameter is a usually a dc resistivity. It has even been mentioned that the results of ac measurements for disordered solids show so much universality that some workers have discontinued work in the field [17, p 877]. It is clear that one sees less detail with the naked eye than with a microscope, suggesting that there might be room in the field of conductive-system analysis for more powerful models than those previously used to reach such a conclusion.

The only IS analysis model known to the present author that allows the direct estimation of appreciably more relevant parameters than the standard approaches is the Poisson–Nernst–Planck (PNP) diffusion one [23–36][4,5,6]. Although it has been theoretically developed since 1953, primarily by the present author and co-authors, it has only been used with complex-nonlinear-least-squares (CNLS) fitting for the analysis of experimental data since 2010, and thus references to earlier background papers on it are relevant. Those by Macdonald may all be accessed and downloaded from the website http://jrossmacdonald.com, available since 2008. Their numbers in the serial list there of Macdonald publications, complete with titles, are appended to the papers cited in the present reference section for easy identification and access. The powerful LEVM CNLS immittance spectroscopy fitting computer program [30] used herein has been freely available since 1990 and has long included many types of fit model, including PNP and PNPA ones.

These models, described in detail in section 2, are of one-dimensional, mean-field, approximate, conductive-system continuum character, involving ordinary (PNP) or anomalous (PNPA) diffusion. They may involve fully blocking electrodes or partial-blocking Chang–Jaffe behavior [23], and/or specific adsorption [28] electrode boundary conditions for ionic or electronic mobile charges. They thus stand in contrast to hopping and trapping percolation discrete-process approaches such as many of those cited in [4–22]. All PNP models satisfy Poisson's equation exactly everywhere between their plane–parallel electrodes, ones here taken identical at both boundaries of the charge-carrying material. Because the PNP work published in the period of 1953–78 was little known, several papers were published thereafter that independently duplicated some of it, but they are not cited here unless relevant.

In section 2, dielectric and conductive-system fitting models and two disparate data sets, used to demonstrate ambiguities, are defined and discussed. Section 3 illustrates the Maxwell ambiguity for both these data sets. Section 4 discusses the remaining ambiguities potentially present for conducting-system models such as the PNPA, and section 5 summarizes conclusions. It should be emphasized that the ambiguities considered here are not in the materials and their data sets but are intrinsic restrictions imposed by our limited models of what particular experimental measurements can tell us about the underlying reality of the material situations.

2. Models, parameters, and data sets used here

2.1. The Havriliak–Negami model and its simplifications

Given a characteristic model relaxation time, τ_0, define the general dimensionless frequency variables $\Omega \equiv \omega\tau_0$; $S \equiv \mathrm{i}\Omega$; and $U \equiv S^{\psi_k}$, with $0 < \psi_k \leq 1$, as used previously in [34, 35]. Then, a general expression for the complex Havriliak–Negami (HN) fitting function may be written as [3]

$$I_k(\omega) \equiv \frac{V_k(\omega) - V_k(\infty)}{V_k(0) - V_k(\infty)} \equiv 1/[1 + U]^{\gamma_k}, \qquad (1)$$

with γ_k usually expected to be no larger than unity. Here I_k is a normalized immittance function that may be defined at the dielectric level for $k = D$ with $V_D(\omega) \equiv \varepsilon(\omega)$, and for $k = C$ at the impedance level with $V_C(\omega) \equiv Z(\omega)$. Then $\Delta\varepsilon \equiv \varepsilon(0) - \varepsilon(\infty)$ is the dielectric strength, and $\varepsilon(\infty)$ will be written hereafter as ε_∞ and is the high-frequency-limiting

[1] The incorrect Eq. (A-12) in this work is corrected in [35].

[2] Add } at right side of equation (9).

[3] The data here were incorrectly treated as specific in character.

[4] See also pp. 4–9, 4–10, 4-26, and 5–15 through 5–19 of the LEVMW manual for discussion of PNP/PNPA models available in the LEVMW fitting program cited in [31].

[5] The newest WINDOWS version, LEVMW, of the comprehensive LEVM fitting and inversion program may be downloaded at no cost by accessing http://jrossmacdonald.com. It includes an extensive manual and executable and full source code. More information about LEVM is provided at this internet address.

[6] Below equation A-1, in γ_j replace θ_j^2 by θ_j, and on p 2279 in t_1 replace ψ by $\psi^{1/2}$.

dielectric constant of the bulk material between electrodes. For $k = C$ we shall take $Z'(0) \equiv R_{\rm dc}$, the dc resistance, or R_0 when the data do not extend to a sufficiently low frequency that $R_{\rm dc}$ may be reliably estimated, and $Z'(\infty) \equiv R_\infty$, with R_∞ often zero. We shall generally consider specific data here, so the normalized quantity $I_C(\omega)$ may then be taken as a normalized impedance, complex resistivity, or other specific immittance [3, see section A.1]. Then, one may define $\rho(\omega) \equiv \rho'(\omega) + {\rm i}\rho''(\omega)$; conductivity level: $\sigma(\omega) \equiv 1/\rho(\omega) \equiv \sigma'(\omega) + {\rm i}\sigma''(\omega)$, and complex dielectric constant level: $\varepsilon(\omega) \equiv \sigma(\omega)/({\rm i}\omega\varepsilon_{\rm V}) \equiv \varepsilon'(\omega) - {\rm i}\varepsilon''(\omega)$, where $\varepsilon_{\rm V}$ is the permittivity of vacuum.

When $\psi_k = \gamma_k = 1$, the HN response function reduces to Debye relaxation at the dielectric level: the DebD model (involving a resistor and capacitor in parallel), and at the conductive-system impedance level, DebC (involving a resistor and capacitor in series). The resulting relaxation times will be termed $\tau_{\rm DD}$ and $\tau_{\rm DC}$, respectively, and replace the general τ_0 quantity used to define the dimensionless frequency-dependent quantities introduced at the beginning of this section and implicit in equation (1). Alternatively, when only $\gamma_k = 1$ the HN reduces to Cole–Cole response, CCD [22] and CCC [14], and when $\psi_k = 1$, Davidson–Cole behavior, designated as DCD [4] or DCC [4, 7, 16]. Note that of the conductive-system HN possibilities, only the DCC Davidson–Cole model for complete blocking involves the physically correct limiting log–log power-law slope of two for $\sigma'(\omega)$ as $\omega \to 0$, as does, of course, its DebC Debye limit. Further, the CCC, sometimes designated the ZC or ZARC, has been shown to be a poor fitting model, and its frequently used real part is even less appropriate [14].

2.2. PNP/PNPA background and response possibilities

References [3, 23–36] are selected continuum ones involving the diffusion of charges. Although the works of Poisson, Nernst, and Planck all greatly predated PNP analysis, it was not until 1953 [24] that it was required that Poisson's equation apply exactly throughout a material with diffusing mobile charge. That PNP analysis was extended in [25–29] and resulted in a very general PNP model [28] that included Chang–Jaffe boundary conditions and parameters [23], essentially equivalent to Butler–Volmer ones for small-signal IS situations, and also possible specific adsorption at the electrodes. In addition, it involved generation–recombination (G–R) effects in which a neutral entity of concentration N_0 partially or fully dissociates into one species of possibly mobile negative charge, n_0, and one of possibly mobile positive charge, p_0, with equal concentrations, c_0. Although we shall take their valence numbers, $z_{\rm n}$ and $z_{\rm p}$, of unity magnitude here (so $\Pi_z \equiv z_{\rm n}/z_{\rm p} = 1$), they may have different mobilities with mobility ratio $\Pi_{\rm m} \equiv \mu_{\rm n}/\mu_{\rm p}$, and even different electrode boundary-condition behaviors.

More history of the development of the PNP and PNPA models is included in [35], but it is worth mentioning that in [29] the PNP model of [28] and some of its limitations are further discussed; further in [31] its predictions for many choices of input variables are illustrated by complex-plane normalized dielectric constant plots; and in [32] the responses of supported and unsupported electroneutral and exact PNP models are compared. Reference [3] explores PNPA anomalous diffusion effects and those depending on G–R parameters, particularly for situations where charges of only one sign are mobile, the one-mobile case, or that where both are equally mobile, the two-mobile $\Pi_{\rm m} = 1$ case. Reference [34] established and verified a simple way to generalize PNP models to PNPA ones and demonstrated further PNPA behavior for three immittance levels. Although the results of [3] and [34] are restricted to completely blocking electrodes, those of [35] compare response equations for several different types of electrode boundary condition, emphasizing partially blocking Chang–Jaffe ones with variable electrode reaction rates. Finally, [36] derived and discussed some more complicated PNPA anomalous diffusion and possible memory effects.

2.3. Summary of PNP/PNPA previous data fittings and two important disparate situations

CNLS fits of data sets for a hydrogel were carried out in [3], while those for the hydrogel, a polymer, and single-crystal $CaCu_3Ti_4O_{12}$ (CCTO) are compared in [34]. All these data sets were found to be best fitted with the charge of a single sign mobile, and they all led to very small dissociation. In [35] it was demonstrated using CCTO data that when the value of the electrode separation, L, was available, fitting led to an estimate of N_0 for the basic material in close agreement with that directly calculated from the structure of the material itself. Here the value of N_0 was many orders of magnitude greater than that of c_0, the estimated mobile charge concentration, a result possibly characteristic of the presence of small nonstoichiometry of the material. Such a response will be designated type A. But another situation where similar small concentrations of mobile charge are present is that where impurity ions or free itinerant electronic charges appear in a solid or liquid material of otherwise purely dielectric character, type B. An example is a water solution with a small amount of NaCl in it. Also for solids, type-B one-mobile behavior with possibly full dissociation of the source of the mobile charges may appear.

The ability of PNP/PNPA data fits to provide direct estimates of N_0 and c_0 is an important strength of these models, one not shared by most others. Often, indirect estimates of N_0 have required estimates of a hopping distance, the Haven ratio, and a hopping rate, and have assumed full dissociation. Such calculations usually involve so many uncertainties in their parameter estimates that the results are likely to be poor.

Data sets exemplifying both type-A and type-B responses are used in the following illustrations of ambiguities: type-A 140 K CCTO data [37], and type-B data for the highly viscous liquid *n*-octylcyanobiphenol in its smectic phase (designated as 8CB) at 301.6 K, kindly provided by Dr Jolanta Świergiel and Professor Jan Jadżyn [38]. Finally, a fit of deionized water data using a fractional diffusion equation of distributed order [36] led to good agreement between that type of

PNPA model and the data [39]. This work also contains an extensive listing of much previous work on diffusion processes, including their [22] citation of 1985 work, probably the first generalization of the Warburg diffusion expression to include an anomalous diffusion fractional exponent of value different from 0.5, as also later mentioned in [34].

A valuable illustration of the use of PNP analysis to estimate ion mobilities in a polymer appeared in 2006 [31] and employed an approximation of the response of the 1953 model of [24]. Since the authors of this work were unaware of the availability of the LEVM complex-nonlinear-least-squares IS fitting model [30] incorporating the full PNP model of [28], they were unable to estimate the mobilities of both charge types and assumed dominant cation mobility, the one-mobile case [3, 34, 35]. Although they were also unable to obtain G–R parameter estimates, they extrapolated to infinite temperature the results of an Arrhenius fit of their estimated cation concentrations to obtain an estimate of the total fully dissociated concentration, essentially the present N_0 quantity, and determined that at their measurement temperatures (0–120 °C) the dissociation was very small. A good summary of other methods of estimating mobility values appears in this paper and some of these methods are described and used in [40], although most alternative approaches do not allow the estimation of the mobilities of charges of both signs from a single set of experimental data, as does the PNP model.

2.4. Limitation of the frequency domain of the one-mobile PNP response

As stated in [18], ergodicity requires that at infinite time (and zero frequency) ions of both signs be mobile (since no potential wells are infinitely deep), but the usual one-mobile definition is experimentally appropriate. In view of practical limitations on the length of experiments and the stability of an experimental material, the one-mobile case is usually well approximated by the mobility-ratio choice of $\Pi_m \geq 10^{15}$, but we shall actually use equivalent values of 10^{38} and 10^{40} to provide discrimination between, and selection of, the two one-mobile models with different free parameters available in the LEVM PNP computer fitting program. A CNLS fit of exact PNP type-A model impedance data with $\Pi_m = 10^{38}$ and a minimum frequency of 0.001 Hz led to a perfect fit quality factor of $S_F \simeq 10^{-13}$, where S_F is the relative standard deviation of the fit residuals. Typical values for excellent fits of experimental data are of the order of 0.01. The other parameters of the model and its important immittance responses are presented in section 3, but here it is useful to explore the effects of fits of the exact $\Pi_m = 10^{38}$ data set with smaller values of this ratio. For simplicity, define the ordinary logarithm of the mobility ratio as KDL [3]. Then for KDL values of 30, 20, 15, and 12, the resulting fit values of S_F are about 10^{-11}, 5×10^{-8}, 5×10^{-3}, and 0.56, respectively.

These values depend, however, on the extent of the low-frequency part of the data, and when the minimum frequency of the data set is decreased to 10^{-5} Hz, for KDL = 30, 20, and 15 they change to about 10^{-10}, 10^{-5}, and 0.42. It is thus clear that the one-mobile approximation becomes poor when the value of KDL is within about nine or ten decades of the minimum frequency of the data. Interestingly, for $\nu_{min} = 0.001$ Hz, CNLS fitting of exact KDL = 12 data at the conductivity level with a fixed value of 38 led to an S_F value of 0.18, with individual real- and imaginary-part values of 0.26 and 0.012. Fitting of these parts separately led to the same value for the real part but to a value of about 10^{-7} for the imaginary part, showing that the deviation was entirely in the real part of the fit, as further confirmed in section 3.

2.5. PNP/PNPA-model expressions and relevant parameters

The Debye length, L_D, is an important element of these conductive-system models. Its general expression is $L_D = L_{D2} \equiv [\varepsilon_\infty \varepsilon_V k_B T/e^2(z_n^2 n_0 + z_p^2 p_0)]^{1/2}$ [3, 28], which may be rewritten here for the uni-univalent situation, where the concentrations n_0 and p_0 are equal to c_0, as $L_{Dj} \equiv [\varepsilon_\infty \varepsilon_V k_B T/je^2 c_0]^{1/2}$ with $j = 1$ or 2. In these expressions e is the proton charge; k_B is Boltzmann's constant; T is the absolute temperature; and $j = 2$ when both charges are mobile in the experimental frequency range, while $j = 1$ when only negative charges are mobile in that range, often the situation for solid materials but not necessarily for liquids. A dimensionless quantity important for IS models and measurements is $M_j \equiv L/2L_{Dj}$ [24, 27, 28], where L is the separation between the plane-parallel electrodes of the measurement cell. For either value of j, M_j is equal to $\varepsilon_0/\varepsilon_\infty$, where ε_0 is the low-frequency-limiting value of the dielectric constant when it exists or when it may be estimated from a good fit of a plausible model [3, 34, 35], and the dielectric strength associated with conductive-system dispersion is defined as $\Delta\varepsilon \equiv \varepsilon_0 - \varepsilon_\infty$.

The equation for the PNP impedance, $Z(\omega)$ (or complex resistivity, $\rho(\omega)$), may be expressed as a combination of a diffusional interface expression, $Z_i(\omega)$, in series with a bulk low-frequency-limiting resistance, $R_0 \equiv 1/G_\infty$, and that combination in parallel with the high-frequency-limiting bulk capacitance, C_∞, as in figure 2(b) of [28]. At sufficiently high frequencies the response reduces to that of R_0 and C_∞ in parallel, and their product is just the Debye relaxation time τ_{DD}, designated τ_D in [3, 34]. In the past, the $Z'(0) = R_0$ plateau value of PNP response for fully blocking electrodes was usually termed R_∞, but this designation is misleading because the model leads to $Z'(\omega) \to 0$ as $\omega \to \infty$. Here the designation R_∞ is reserved for a possibly present series resistance not an intrinsic part of the model. Further, R_0 is only the dc resistance in the limit of zero blocking: so-called transparent electrodes [35].

All PNP models involving ordinary diffusion may be readily generalized to incorporate anomalous diffusion in their interface responses by the introduction of a new fractional-exponent Warburg-type parameter, $\psi (0 < \psi \leq 1)$ [34]. They are then designated as PNPA ones when $\psi < 1$. The parameter ψ then induces power-law behavior in the low-frequency immittance interface response regions. Now, on introducing the additional dimensionless variables $P \equiv p^2 \equiv 1 + U \equiv 1 + (i\omega\tau_{DD})^\psi$ in addition to those defined in section 2.1, we may define the important fractional-exponent,

diffusion-related dimensionless quantity $Q \equiv \tanh(q)/q$, with $q \equiv pM_j$. Since $p \equiv [1 + U]^{0.5} \equiv [1 + S^{\psi}]^{0.5}$, we see that for $\psi = 1$, the ordinary diffusion case, $Q = Q_1 \equiv \tanh[M_j(1+\mathrm{i}\omega\tau_{\mathrm{DD}})^{0.5}]/[M_j(1+\mathrm{i}\omega\tau_{\mathrm{DD}})^{0.5}]$ reduces to a form of ordinary Warburg diffusion when $\omega\tau_{\mathrm{DD}} \gg 1$. For $\omega \to 0$, $Q \to \tanh[M_j]/[M_j]$, closely equal to $1/M_j$ for $M_j \geq 5$.

Transformation from raw impedance data represented by $Z(\omega)$ to specific data at the same immittance level involves just $\rho(\omega) \equiv 1/\sigma(\omega) \equiv \mathrm{CC} \times Z(\omega)$, where the cell constant $\mathrm{CC} \equiv A/L$ and A is the area of an electrode, often taken as of unit area in much of the earlier theoretical PNP work. The expressions for σ_∞ and ε_∞ in the present PNP case are $ec_0\mu_{\mathrm{n}}(1 + \Pi_{\mathrm{m}}^{-1})$ and $[\sigma''(\omega)/(\varepsilon_{\mathrm{V}}\omega)]_{\omega\to\infty}$, respectively. Further, the general τ_0 of the dimensionless frequency variable Ω and the others defined at the beginning of section 2.1 involve the PNP τ_{DD} characteristic relaxation time.

As shown in [3, figure 4], the generation–recombination (G–R) process, involving dissociation of a neutral entity, N_0, into possibly mobile positive and negative charges of equal concentrations, c_0, can lead to a relatively narrow range of dissociations that produces low-frequency plateaus in $Z'(\omega)$ appearing at lower frequencies than the usual PNP one of height R_0. This interesting effect has, however, not been apparent in any of the experimental data sets so far fitted with the PNP approach. Instead, such data, including those considered herein, are found to be best fitted by the charge of only a single sign mobile and either small or full dissociation. The degree of dissociation, $D_{\mathrm{D}} \equiv c_0/N_0$, is determined by a quadratic equation [3, equation 1] which involves the ratio of a generation parameter and a recombination one, k_{gr}, of dimension cm^{-3} in cgs units, used herein. For $D_{\mathrm{D}} \ll 1$, the quadratic reduces to $c_0 \cong [k_{\mathrm{gr}}N_0]^{0.5}$, applying for $k_{\mathrm{gr}} \ll N_0$. Although the usual PNPA model with Chang–Jaffe electrode boundary conditions has been identified as CJPNPA in [35], we shall just use the designation PNPA here to include the possibility of partial blocking and omit consideration of specific adsorption [28]. As shown in that reference, the two possibly non-zero dimensionless CJ electrode reaction rates for positive and negative charges are defined as ρ_j, and are not resistivities. They are related to the actual reaction rates by $k_j = (2/L)D_j\rho_j$, of dimension cm s^{-1}, and the charge mobilities, of dimension $\mathrm{cm}^2\ \mathrm{V}^{-1}\ \mathrm{s}^{-1}$, are related as usual to diffusion coefficients by $\mu_j = (e/k_{\mathrm{B}}T)D_j$.

In uni-univalent PNPA fits, the following parameters are usually taken fixed with known values: A, L, and T. Possibly free parameters may include N_0, k_{gr}, ρ_j (the normalized electrode reaction-rate parameters), Π_{m} , μ_j or ρ_0, ε_∞, and ψ. Other parameter values, such as those of c_0, the μ_js and D_js, $L_{\mathrm{D}j}$, and M_j, are calculated from fit results. The normalized impedance is $Z_{\mathrm{TN}} = Z_T/R_0 = \rho_{\mathrm{TN}} \equiv \rho_T/\rho_\infty$ and may be related to its interface part, Z_{iN}, that does not include the bulk quantities ρ_∞ and ε_∞, by the relation

$$Z_{\mathrm{TN}} = 1/[S + 1/(1 + Z_{\mathrm{iN}})] \tag{2}$$

and its inverse

$$Z_{\mathrm{iN}} = [(1 + S)Z_{\mathrm{TN}} - 1]/[1 - SZ_{\mathrm{TN}}]. \tag{3}$$

An expression for the impedance of the full general PNP model, including arbitrary mobilities, G–R effects, and CJ electrode reaction rates, is given in [28]. Although it and its PNPA generalization [30, 34, 35] are too long and complicated to list, they are included in Circuit H of the free LEVM computer program, available for fitting experimental data and generating synthetic data [30]. For the data fittings required here it is sufficient to list here the expression for partial blocking PNP one-mobile response with small dissociation [35], noting that the first glimmer of ambiguity occurs in [28] where it is shown that for full blocking the equal mobility expression with full dissociation is of the same general form as that of the one-mobile situation. The one-mobile PNP model with small or full dissociation may be expressed for $M = M_1$ as [35, equation 7]

$$Z_{\mathrm{TN}} = [(S + Q_1) + P_1Q_1\rho_2]/[(SP_1) + P_1^2Q_1\rho_2], \tag{4}$$

consistent with the fully blocking ($\rho_2 = 0$) PNPA result of equation (6) of [34] for $\psi = 1$. Equation (4) may be generalized by using equations (3) and (4) to obtain Z_{iN} and then applying the procedure of [34] to obtain the corresponding PNPA result.

3. PNP/PNPA exact immittance responses for three mobility ratios

Most of the ambiguities considered in the next sections involve mobility values of positive and negative charge carriers: possible parameters of the PNP/PNPA IS response models, but not of most others. Therefore, it is worthwhile, before comparing the responses of the type-A and -B experimental data sets, to show some exact predictions of these models for the limiting values of $\Pi_{\mathrm{m}} = 1$ and 10^{38} and the intermediate case of 10^5. We thus show PNP/PNPA-model responses similar to those found on fitting $CaCu_3Ti_4O_{12}$ data in [35] except that fully blocking electrodes are here assumed. Some of the type-A, one-mobile parameter values used were $N_0 = 2 \times 10^{20}$ cm^{-3}; $k_{\mathrm{gr}} = 10^5$ cm^{-3}; and $n_0 = p_0 \equiv c_0 \cong 4.472 \times 10^{12}$ cm^{-3}, showing a very small-dissociation value well approximated by $n_0 \cong [k_{\mathrm{gr}}N_0]^{1/2}$ [35]. The quantity ξ, the ratio of the recombination relaxation time to the Debye relaxation time, here designated τ_{DD}, was set as usual to 10^{30} to avoid recombination in or near the available frequency range [3]. In addition, other T, L, ρ_0, ε_∞, τ_{DD}, μ_{n}, and M_1 values were 140 K, 0.1 cm, 1.396×10^5 Ω cm, 100, 1.236×10^{-6} s, 10 cm^2 ($\mathrm{V}^{-1}\ \mathrm{s}^{-1}$), and 129.5, respectively. The frequency ν_{h} corresponding to the PNP τ_{DD} value is then about 1.29×10^5 Hz here.

Figure 1 shows full CNLS $\varepsilon'(\nu)$ responses of the PNP model calculated in each case with all model parameters the same except for three different KDL = 0, 5, and 38 fixed values. The figure 1(a) linear–log plots well demonstrate the KDL = 5 transition from the one-mobile value of $\varepsilon_0 = (\varepsilon_0)_1$ to the two-mobile one with $\varepsilon_0 = (\varepsilon_0)_2 \to \sqrt{2}(\varepsilon_0)_1$. In addition, figure 1(b) includes both ε' and ε'' log–log PNP responses for both $\varepsilon'(\nu)$ and $\varepsilon''(\nu)$, as well as PNPA responses for $L = 38$. Figure 2 presents dielectric-level complex-plane plots corresponding to the results of figure 1 and, as well, part

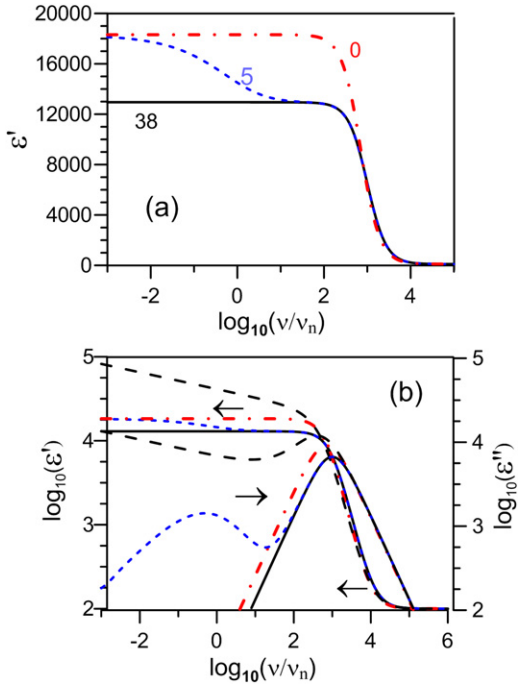

Figure 1. Linear–log PNP-model plots of $\varepsilon'(\nu)$ for the three values of KDL $\equiv \log_{10}(\Pi_m)$: 0 (dash–dot), 5 (short dash), and 38 (solid), here covering the mobility range from $\mu_n = \mu_p = 10$ cm^2 (V^{-1} s^{-1}), to $\mu_n = 10$ cm^2 (V^{-1} s^{-1}), $\mu_p = 10^{-4}$ cm^2 (V^{-1} s^{-1}), and $\mu_n = 10$ cm^2 (V^{-1} s^{-1}) and $\mu_p = 10^{-37}$ cm^2 (V^{-1} s^{-1}). (b) Log–log plots of PNP $\varepsilon'(\nu)$ response (left y-axis) and $\varepsilon''(\nu)$ response (right y-axis), and PNPA real- and imaginary-part results for $L = 38$ with $\psi = 0.9$ (long dashes). Here and elsewhere $\nu_n = 1$ Hz, and the arrows in part (b), and figures 3 and 4 show which responses are associated with the left and which with the right axis scales.

of the KDL $= 38$, $\psi = 0.9$ response. This, and the KDL $= 5$, $\psi = 0.9$ responses, are also shown with a different $\varepsilon'(\nu)$ scale, at the top, to include more of their low-frequency responses, at the sacrifice of equal x- and y-axis scales, the usual choice for complex-plane plots.

Figure 3 shows type-A $\rho(\nu)$ and $\sigma(\nu)$ exact calculated results extended to lower frequencies in order to show the beginning of the KDL $= 5\rho'(\nu)$ low-frequency plateau. It is clear that although the KDL $= 0$ and 38 results for $\rho'(\nu)$ are identical, small differences begin to appear between the other curves at frequencies less than about 10^5 Hz. A publication entitled 'one sign ion mobile approximation', that deals with type-B PNP mobility effects of fully dissociated positive and negative charges has recently appeared [41]. Its exact theoretical results are somewhat similar to those shown here, although its results are not in specific form and no dielectric responses are presented.

Reference [41] shows, as expected, that the frequency, ν_h, at which $Z'(\nu)$ or $\rho'(\nu)$ begins to decrease for the two-mobile KDL $= 0$ situation involves free diffusion and is mediated by the Debye relaxation time. In addition, it presents an expression for the frequency, ν_l, at which the low-frequency plateau begins to appear for intermediate values of KDL and relates it to ambipolar diffusion, implicit in the original PNP work [24], as discussed in [32, equation 24].

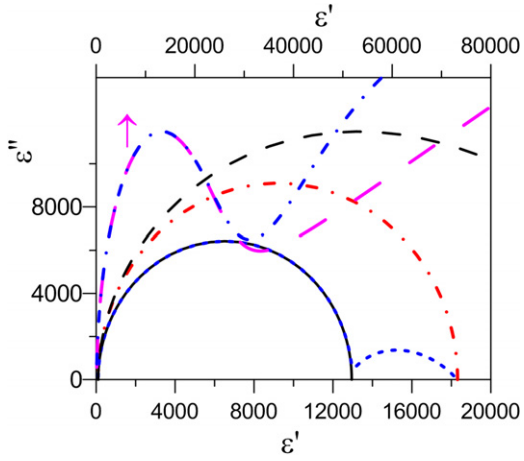

Figure 2. Complex-plane plot of the PNP-model responses of figure 1. In addition, the long-dashed line is that for the low-frequency part of the PNPA response with KDL $= 38$ and $\psi = 0.9$. The next two lines involve the upper ε' scale. The lower-slope one on the right, for KDL $= 38$ and $\psi = 0.9$, uses very long dashes, and the middle one, for KDL $= 5$ and $\psi = 0.9$, involves a dash–dot line.

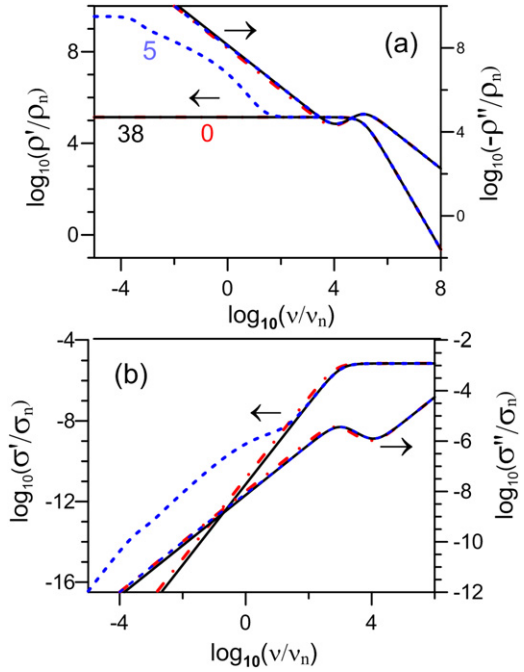

Figure 3. Log–log PNP-model responses with extended low-frequency ranges for the three mobility ratios with the same KDL line choices as in figure 1(a). (a) $\rho(\nu)$ response: real part, left y-axis; imaginary part, right y-axis. (b) $\sigma(\nu)$ response: real part, left y-axis; imaginary part, right y-axis. Here and elsewhere $\sigma_n = 1$ S cm^{-1} and $\rho_n = 1$ Ω cm.

Finally, [41] discusses the minimum and maximum values of $-Z''(\nu)$ (here $-\rho''(\nu)$ for the present specific data, as in figure 3(a)), which often appear in log–log resistivity plots. Such minima and maxima of resistivity, conductivity, and dielectric plots are illustrated for the Davidson–Cole DCC response model in [3, figure 7]. For $-Z''(\nu)$ response, its maximum occurs at ν_h, but the minimum is defined in [41] to occur at the lower frequency, ν^*. In equation (46)

Table 1. CNLS fits with proportional weighting of the dielectric-system and conductive-system models of smectic liquid n-octylcyanobiphenol (identified as 8CB herein) at 301.6 K, and of single-crystal $CaCu_3Ti_4O_{12}$ (CCTO, identified as CC below) at 140 K, specific data sets at the $\varepsilon(\nu)$ immittance level. In the heading of column 1, 'TYP' specifies either type-A intrinsic or type-B extrinsic: partly or fully dissociated conduction when appropriate. The dielectric-system models used here are DebD, DCD, and CGDebD, while the conductive-system ones are C(R · DebC), PNP, and PNPA. The composite model CGDebD involves a dielectric Debye model in parallel with a capacitance and conductance, while the C(R · DebC) one consists of a conductive Debye model in series with a resistance and the combination in parallel with a capacitance. Percentage values are listed for the goodness-of-fit parameters, S_F (the relative standard deviation of the fit residuals), and P_F (the rms value of the relative standard deviations of the free parameters of a fit, PDRMS). All parameter values shown are free except those marked 'F' for fixed, and those marked 'C', calculated from other fit parameter values. The PNP/PNPA one-mobile, KDL = 38 models used for CNLS fitting with the LEVMW program involve either ρ_∞ or μ_n free, but not both simultaneously. The symbols and values enclosed in braces are alternates to ones without enclosure. All units are in cgs here; thus the units of ρ_∞ and ρ_D are Ω cm.

#/TYP/MAT/ MODEL	S_F/P_F (%)	ε_∞ L	$\Delta\varepsilon$ ε_0	$10^8\tau_{DD}$	ψ	$10^{-4}\rho_\infty$ $\{\rho_2\}$	k_{gr} $\{10^{-7}\rho_D\}$	N_0 c_0	μ_n	μ_p	KDL M_1
1/B/8CB/ DebD	2.52 0.50	3.29 0.01F	10.84 14.13C	5.02C	1F						
2/B/8CB/DCD	1.47 0.46	3.19 0.01F	10.85 14.03C	5.42C	0.943						
3/B/8CB/C(R· DebC)	1.84 7.88	3.29 0.01F	— —	6145C	1F	5.18 —	— {6.47}				
4/B/8CB/ PNP	2.11 0.52	3.26 0.01F	10.79C 14.05C	1.37C	1 F	4.73 —	10^{35}F —	3.51×10^{10} 3.51×10^{10}C	3762C	—	38F 4.33C
5/B/8CB/ PNPA	1.23 0.31	3.25 0.01F	10.71C 13.96C	1.34C	0.995	4.65 —	10^{35}F —	3.37×10^{10} 3.37×10^{10}C	3978C	—	38F 4.25C
6/A/CC/PNP	1.86 28.7	417 0.11F	1.92×10^5C 1.93×10^5	4.82C	1F	0.1305 {0.0341}	2.59×10^6 —	1.48×10^{22}F 1.96×10^{14}C	24C	— —	38F 461C
7/A/CC/PNPA	1.67 5.18	174 0.11F	7.72×10^4C 7.74×10^4C	2.01C	0.909	0.1304 {0.0324}	3.90×10^5 —	1.458×10^{22}F 7.59×10^{13}C	63C	— —	38F 445C
8/A/CC/ CGDebDEx	10^{-8} 10^{-7}	174 0.11F	7.24×10^4 7.26×10^4C	864C	1	4.160* —					

of [42], an interesting and novel expression connecting these two frequencies is presented. It may be re-interpreted and rewritten in the present notation as $\nu_h/\nu^* = \sqrt{M_j}$, and should, in fact, apply to the corresponding maxima and minima that appear in the resistivity, conductivity, and dielectric responses for appropriate conductive-system models such as the DCC and the PNP. Using the LEVM program to generate many exact data points around the minima and maxima regions for PNP data involving a specific M_1 or M_2 value, one may calculate very accurate values of the above ratio. The maximum disappears for M of the order of 10 or smaller, but one finds that its value calculated from the above expression is about 14% too small for $M = 25$ and about 7% too small for $M = 129.4$. Evidently, the equation is asymptotically more and more appropriate for larger values of M. It should, nevertheless, be of some value as one way of estimating M from experimental data, since for usual data where often $100 < M < 1000$ the above ratio is unlikely to lead to estimates direct from the data of better than 5% or so.

Figure 4 presents IS data for the two different materials that are used in the subsequent demonstrations of ambiguities that may arise in the fitting of frequency response data to models. The CCTO material is a single-crystal solid with gold-sputtered electrodes and 23 data points. The results of its type-A, 140 K PNPA data fits are discussed in [35]. In contrast, we also fit 47-point, type-B n-octylcyanobiphenol (8CB) data at 301.6 K. It is a member of the cyanobiphenyl family and gold-plated electrodes were used [38]. The electrode separations of the two materials were 0.11 cm for the first and 0.01 cm for the second. Their fit parameter values

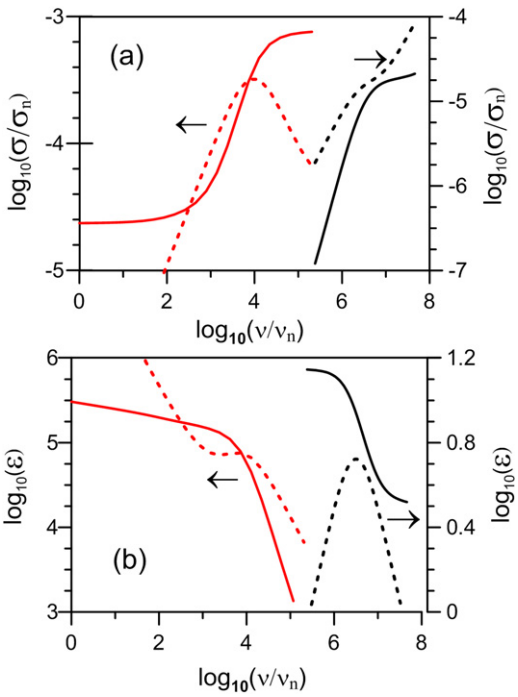

Figure 4. Log–log experimental data responses for (a) $\sigma(\nu)$ and (b) $\varepsilon(\nu)$. Type-A 140 K CCTO response on the left using the left y-axis, and type-B 301.6 K 8CB response on the right using the right y-axis. Real parts: solid lines, imaginary parts: dashed lines.

are listed in the tables in the following sections, and the best fits were sufficiently accurate that the data and fit values are virtually indistinguishable in the log–log plots of figure 4.

4. The Maxwell ambiguity (#1) (table 1)

We start with obvious or well-known ambiguities and progress to less familiar or new ones. Since the ambiguities considered are present both for fully blocking and for partial blocking of mobile charges at the electrodes, we consider here data sets involving both possibilities. Ambiguity #1 demonstrates the well-known fact that external measurements do not allow discrimination between conduction and displacement current effects [2, 3]. It is therefore designated as the displacement–conduction or dielectric–conduction ambiguity (DCA). All ambiguities discussed here are symmetrical, so DCA = CDA.

Comparison of the 8CB dielectric-model results in row 2 of table 1 with those of the one-mobile PNPA conductive-system fit of row 5 shows that their fits are not only comparable but excellent. Here the important fit quality factors, S_F and P_F, whose values are listed in tables 1 and 2, are defined in the caption of table 1. For the 8CB data set it was not possible to find meaningful estimates of N_0 and the highly correlated generation–recombination parameter, k_{gr}, when both were free, so k_{gr} was fixed at a very large value to ensure no recombination in the time scale of the experiment, leading to a small estimate for N_0 and to full dissociation, type-B behavior. This choice is further discussed in section 5.

We see that changing from the dielectric Debye model of row 1 to the Davidson–Cole DCD one of row 2 improves the fit appreciably, suggesting the presence of some fractal effects in the dielectric dispersion [16]. Similarly, the change from ordinary diffusion in the PNP results of row 4 to the anomalous diffusion PNPA behavior of row 5 also leads to an appreciably better fit, even though the value of the ψ parameter of the latter remains very close to unity. Finally, the large $P_F \equiv$ PDRMS value for the conductive-system composite Debye fit of row 3, primarily involving the uncertain DebC parameter estimates, demonstrates that the PNP and PNPA models are far more appropriate here than is the DebC one. Although the present fits of the 8CB data well demonstrate the Maxwell or dielectric–conductive-model ambiguity (DCA), the extremely high mobility estimates found from the conductive-system-model fits suggest the unlikely presence of itinerant highly mobile electronic charges that are nevertheless fully blocked at the electrodes. Thus, without a plausible explanation for the presence of such charges, the ambiguity must be resolved in favor of pure dielectric dispersion, as in rows 1 and 2, and consonant with the original experimental analysis of the 8CB data [38].

Rows 6–8 show one-mobile fit results for the CCTO data set. This is a challenging but interesting set because it involves partial blocking of charges at the electrodes, appreciable anomalous diffusion, and high-frequency response so limited that no approach to an ε_∞ value is evident in figure 4. It is of type-A character, and N_0 is here fixed at the known intrinsic material value estimated and discussed in [35]. Although again the PNPA fit is much superior to the PNP one, the limited data range leads to an appreciably larger value of PDRMS even for the PNPA fit. Further, for all the PNP and PNPA results shown in the table, even for the PNPA one of row 7 involving the dimensionless reaction-rate parameter, ρ_2 (whose values are shown in rows 6 and 7), the $\Delta\varepsilon$ and ε_0 values all apply to those arising from the PNP model with full blocking of charges at the electrode. Therefore, although the M_1 results listed in table 1 were calculated as usual from $L/2L_{D1}$, they were also here equal to the $\varepsilon_0/\varepsilon_\infty$ ratio value [35].

Finally, to investigate the possibility of mobile charges of both signs, all PNP and PNPA fits were carried out with different fixed values of KDL, with k_{gr} free or with both free. Worse fits were found for $0 <$ KDL < 10, and those greater than 10 were identical to those with 38. See section 5 for analysis of the two-mobile, equal mobility situations with KDL = 0. In the table, mobility values less than 10^{-15} are taken as zero and omitted, as is also the case for all the μ_p ones here for KDL = 38.

It was not found possible to obtain an adequate dielectric-model fit of even exact, extended range data calculated from the parameters of row 7, primarily because of its appreciable anomalous diffusion resulting in the continuously increasing $\varepsilon(\nu)$ at low frequencies, as shown in figure 4(b). Therefore, the row 7 parameters with ψ fixed at unity were used with its original limited frequency range to generate exact PNP data. It could be fitted exactly with the composite dielectric DebD model of row 8. Its ρ_∞ value is marked with an asterisk to indicate that this fit value is actually the inverse of the free parallel σ_P parameter designated by G in the model name. Again, the Maxwell DC ambiguity is fully confirmed, but this time it is clear that CCT0 involves electronic conduction with charge mobility much too high to arise from mobile ions [35], and the observed dispersion involves anomalous charge diffusion and not dipolar dielectric dispersion.

5. Additional ambiguities (table 2)

We consider here the remaining five ambiguities. They are of the following character: given a good or perfect fit of an experimental or exact data set, change and fix the value of one parameter of the model and then fit it with that one parameter fixed but with a few or all of the other originally free ones again free. Ambiguity is evidenced if the resulting fit is sufficiently comparable to the original one that it is then impossible to make a plausible choice between them based on such fit results. In a recent paper dealing with statistical errors, the authors said 'What seem like natural calculations are stymied by the impracticability, in real life, of changing one variable while leaving all other variables constant' [42]. This is, however, essentially the situation exemplified by the results of figure 3 where three different values of KDL were used to compare the resulting changes in exact PNPA-model responses. Here, however, we deal with restricted real-life situations where a single fit parameter of a given model is changed from its original value and fixed at a different value, and then the same data set is again fitted with the same model. If the fit quality is identical to or practically indistinguishable

Table 2. CNLS fits with proportional weighting of conductive-system PNPA models of single-crystal $CaCu_3Ti_4O_{12}$ (CCTO, identified as CC below) at 140 K, specific data sets at the $\varepsilon(\nu)$ immittance level; compare table 1, row 7, one-mobile results. In the heading of column 1, '#' designates the ambiguity number; 'TYP' here specifies type-A intrinsic or type-B extrinsic: partly or fully dissociated conduction; and the ambiguity designations are explained in the text. The other items are the same as in the heading of table 1. In rows 4a, 5a, and 6a only two parameters are free and they are shown in boldface.

#/TYP/MAT/ MODEL/ambiguity designation	S_F/P_F (%)	ε_∞ L	$\Delta\varepsilon$ ε_0	$10^8\tau_{DD}$	ψ	$10^{-4}\rho_\infty$ ρ_2	k_{gr}	N_0 c_0	μ_n	μ_p	KDL M_1
2/A/CC/PNPA/ CSSA	1.67 5.18	174 0.11F	7.72×10^4C 7.74×10^4C	2.01C	0.909	0.1304 0.0324	3.90×10^5	1.48×10^{22}F 7.59×10^{1}3C	—	63C	**−38F** 445C
3/B/CC/PNPA/ABA	1.67 3.59	174 0.11F	7.72×10^4C 7.74×10^4C	2.01C	0.909	0.1304 0.0324	**10^{35} F**	7.59×10^{13} 7.59×10^{13}C	63C	—	38F 445C
4a/A/CC/PNPA/ 12LA	4.05 1.08	174F **0.074**	7.38×10^4C 7.39×10^4C	2.01F	0.909F	0.1304F **0.0660**	3.90×10^5F	1.48×10^{22}F 7.59×10^{13}C	31.5C	31.5C	0F 426C
4b/A/CC/PNPA/ 12LA	2.11 2.67	225 0.079	7.72×10^4C 7.74×10^4C	2.62	0.924	0.1312 0.0675	3.90×10^5F	1.48×10^{22}F 7.59×10^{13}C	31.3C	31.3C	0F 396C
4c/A/CC/ PNP/12LA Ex	10^{-8} 0.001	174 0.078	7.72×10^4C 7.74×10^4C	2.01C	1	0.1304 —	3.90×10^5F	1.48×10^{22}F 7.59×10^{13}C	31.5C	31.5C	0F 445C
5a/A/CC/PNPA/ 12kgA	4.05 2.52	174F 0.11F	7.38×10^4C 7.39×10^4C	2.01F	0.909F	0.1304F **0.0660**	**8.12×10^4**	1.48×10^{22}F 3.47×10^{13} C	69C	69C	0F 426C
5b/A/CC/PNPA/ 12kgA	2.11 5.21	225 0.11F	8.91×10^4C 8.93×10^4C	2.62	0.924	0.1312 0.0675	1.03×10^5	1.48×10^{22}F 3.90×10^{13}C	61C	61C	0F 396C
5c/A/CC/PNP/ 12kgA Ex	10^{-8} 0.001	174 0.11	7.72×10^4C 7.74×10^4C	2.01C	1	0.1304 —	9.74×10^4	1.48×10^{22}F 3.80×10^{13}C	63C	63C	0F 445C
6a/A/CC/PNPA/ 12N0 A	4.05 2.52	174F 0.11F	7.38×10^4C 7.39×10^4C	2.01F	0.909F	0.1304F **0.0660**	3.90×10^5F	**3.08×10^{21}** 3.47×10^{13}C	69C	69C	0F 426C
6b/A/CC/PNPA/12 N0 A	2.11 5.21	225 0.11F	8.91×10^4C 8.93×10^4C	2.62	0.924	0.1312 0.0675	3.90×10^5F	3.91×10^{21} 3.90×10^{13}C	61C	61C	0F 396C
6c/A/CC/PNP/ $12N_0$ A Ex	10^{-8} 0.001	174 0.11	7.72×10^4C 7.74×10^4C	2.01C	1	0.1304 —	3.90×10^5	3.70×10^{21} 3.80×10^{13}C	63C	63C	0F 445C

from that of the original, then the model is ambiguous for that parameter.

We illustrate the following ambiguities primarily using the one-mobile, row 7, CCTO PNPA fit of table 1. Therefore, the fit results in table 2, involving different mobility situations, should be compared to that one. Ambiguity #2 just summarizes the charge-sign symmetry (CSSA) of most if not all IS models. With KDL = −38 (shown in boldface) rather than the 38 of row 7 we see that the μ_n and μ_p values are just reversed. Thus, the fit results are the same for KDL positive or negative, whether the charge of one sign has a higher mobility and the other one a lower mobility or exactly vice versa. The matter is, of course, moot when KDL = 0 and thus $\Pi_m = 1$. When the mobilities are different, external information is necessary to help decide which charge type is which. But fits with $\Pi_m < 1$ are unnecessary because of charge-sign symmetry when $\Pi_z = 1$.

Ambiguity #3 is that between type-A and type-B intrinsic–extrinsic models and may be designated as ABA. When k_{gr} is fixed at a very large value (shown in boldface in table 2), the resulting fit with N_0 taken free leads, for both it and c_0, to the same small c_0 value as that in row 7 but here a full-dissociation one, as well as the same or better fit quality values. Thus one also needs external information about the material involved to resolve this ambiguity [35]. When the above process is carried out in reverse, however, beginning with the table 1, row 5 8CB fit results, one finds that, starting with any fixed value of $N_0 \geq c_0$ and allowing k_{gr} to be free to vary, the resulting fit value of k_{gr} leads again to just the same estimate of c_0. For this case, it is evidently impossible to find a unique estimate of N_0; this is not surprising since the 8CB data are best interpreted as being of virtually pure dielectric character.

The remaining ambiguities all involve fixed two-mobile KDL = 0 PNP/PNPA situations and should be compared with the one-mobile results of row 7 in table 1. Their designations are of the form $12xA$, where x is the only or principal free parameter in the two-mobile fits. Although the normalized electrode reaction rates, ρ_1 and ρ_2, might both be non-zero in the two-mobile case, for simplicity we set $\rho_1 = 0$, so positive mobile charges are then completely blocked at the electrodes. For each of the following ambiguities we show PNPA limited data fit results with minimum free parameters and also with all original parameters free except when the correlations between two parameters are ±1 and preclude proper fits of both free together. For example, the exact data correlations between L and k_{gr}, N_0 and k_{gr}, and L and N_0 are here −1, −1, and 1, respectively. In addition, three fit results, marked 'Ex' in the ambiguity designations of column 1, are shown for exact PNP fully blocking data extending from 10^{-3} to 10^8 Hz. They show exact, ideal parameter changes produced by fixing a minimal number of parameter values. These data sets were calculated using the parameter values of row 7 of table 1 except with $\Pi_m = 1$, $\psi = 1$, and $\rho_2 = 0$.

Here ambiguity #4, designated 12LA, involves L taken free to vary. But since the actual electrode reaction rate is

$k_j = (2/L)D_j\rho_j$, for incomplete blocking it is necessary to allow ρ_2 to be free as well to avoid a change of L affecting k_2, a quantity which should not depend on L except possibly when $M < 3$. The values of k_2 following from those in lines 4a and 4b of table 2 and line 7 of table 1 are about 0.68, 0.65, and 0.45, respectively, not remarkably similar. Nevertheless, the fit quality results for these three fits well demonstrate the presence of the 12L ambiguity, and we see that the two-mobile equal mobilities are closely or exactly one-half of the one found for the one-mobile fit.

Finally, ambiguities #5 and #6 are generally more serious than #4 because there a good value of L is usually known, usually not the case for k_{gr} and N_0. The ambiguity #5 results are very similar to those for #4 except that initially k_{gr} and ρ_2, rather than L and ρ_2, are free to vary, and the c_0 and μ_j values are respectively about one-half smaller and twice larger than those of #4. Here either L or N_0 may be taken free to vary but not both at the same time. For ambiguity #6 with N_0 free to vary, all relevant parameters may, however, be taken simultaneously free for the PNP exact data fit. Incidentally, the values of the PDRMS fit estimates for the three PNP fits are relatively larger than might be expected for exact data, particularly because of the high correlations between the parameters mentioned above. When one or more of them are fixed, the PDRMS values then become of the order of 10^{-8}% or less. Note that when differences in the values of the two-mobile parameters from those of the one-mobile ones appear, their ratios are ideally $\sqrt{2}$, 2, or 4, values readily explained from expressions such as those for M_j and ρ_∞.

Table 3. Except for ambiguities #s 1–3, an exact data set calculated from a one-mobile ($\Pi_m = 10^{38}$) fully blocking PNP model is fitted using CNLS with proportional weighting by the same model but set for the two-mobile, equal mobility condition ($\Pi_m = 1$), and the changes induced in the relevant parameters listed in column two are shown in column three. Note that all ambiguities are reversible so, for example, DCA and CDA both apply.

A#	Ambiguity designation and model fit examples in rows of tables 1 and 2 (Tx:RyRz)	A. Input model and relevant parameters	B. Ambiguous fitting results of the A-model data
1	DCA T1:R1R2; T1:R7R8	Any good fitting model of pure dielectric response	Any good conductive-system fitting model of the dielectric data in A
2	CSSA T1:R7; T2:R2A	PNP or PNPA $\Pi_m : \mu_n, \mu_p$	PNP or PNPA $1/\Pi_m : \mu_n \to \mu_p$, and $\mu_p \to \mu_n$
3	ABA T1:R7; T2:R3A	PNP or PNPA $k_{gr} \ll N_0$ and $N_0 \gg c_0$	PNP or PNPA $k_{gr} \gg N_0$ and $N_0 = c_0$
4	12LA T1:R7; T2:R4aA4bA4cA	PNP $\Pi_m = 10^{38}$ L, μ_n	PNP $\Pi_m = 1$ $L/\sqrt{2}$, $\mu_n/2$
5	$12k_{gr}$A T1:R7; T2:R5aA5bA5cA	PNP $\Pi_m = 10^{38}$ k_{gr}, c_0	PNP $\Pi_m = 1$ $k_{gr}/4$, $c_0/2$
6	$12N_0$A T1:R7; T2:R6aA6bA6cA	PNP $\Pi_m = 10^{38}$ N_0, c_0	PNP $\Pi_m = 1$ $N_0/4$, $c_0/2$

6. Summary and conclusions (table 3)

Since an appreciable amount of the PNP work published in the 1953–88 period was evidently not well known and was independently duplicated later, brief summaries of some of the early work and of early and later data fitting using PNP and PNPA models have been included herein. To possibly help ameliorate this problem, since 2008 all the publications of the present author have been listed and made available on the website http://jrossmacdonald.com.

The six ambiguities described in sections 4 and 5 involve experimental data of dielectric and conductive-system character. The first three are basic and of general applicability, but the remaining three apply only to situations where the concentrations of charges of both signs are equal, because of partial or full dissociation from a neutral entity, and, as well, they have exactly equal mobilities. Although this is, in principle, a real-life possibility, this mobility-equality restriction is highly unlikely, even for liquids. It should now be clear that the title of this work applies first to the three basic ambiguities and only second to the remaining three involving KDL = 0 response.

Theoretical analyses that assume the presence of equal mobilities for positive and negative charges (e.g., [34, 39, 43]) might seem to be of much less practical value than those that allow arbitrary values of the mobility ratio. But two-mobile ambiguities involving equal mobility values, which apply to type-B (see ambiguity #3) as well as to type-A situations, show that the results of unlikely KDL = 0 theoretical and experimental approaches may be re-interpreted as representing actual one-mobile situations, with the assumed or estimated KDL = 0 model parameters readily changed, using the results of the more likely one-mobile case. Further, the present results imply that, even for PNP and PNPA ambiguous KDL $\gg$ 1 and KDL = 0 theoretical and experimental results, it is always sufficient to assume KDL $\gg$ 1 rather than KDL $\ll$ 1. When PNP/PNPA fits of experimental data with Π_m free to vary lead to intermediate values of KDL greater than zero and less than large values such as 20, however, one may again still need to rely on external knowledge of the experimental situation and possibly results of different experiments to resolve any remaining ambiguities.

A summary of all six ambiguities is provided in table 3, where their ideal parameter changes are illustrated by fits of exact PNP data extending from 10^{-3} to 10^{8} Hz. These ideal values may be compared to the approximate ones of table 2 found by fitting actual experimental data; see the examples listed in column 2 of table 3. In column 3 a model is identified, along with those of its parameters relevant to the ambiguity considered and taken free to vary in fits of its data. Finally, for ambiguities 4–6 column 4 shows the resulting changes in the free parameters on fitting the data of the model in column 3 with the KDL = 0 two-mobile restriction.

Acknowledgments

It is a pleasure to thank Professor Jan Jadżyn and Drs Jolanta Świergiel and Peter Lunkenheimer for providing

the experimental data sets used herein and for useful discussions. I also thank the referees for valuable comments and suggestions.

References

[1] Havriliak S and Negami S 1967 *Polymer* **8** 161
Havriliak S and Negami S 1994 *J. Non-Cryst. Solids* **172–174** 297
[2] Macdonald J R 1999 *Braz. J. Phys.* **29** 332
[3] Macdonald J R 2010 *J. Phys.: Condens. Matter* **22** 495101
See also Derfel G, Lenzi E K, Yednak C R and Barbero G 2010 *J. Chem. Phys.* **132** 22401
[4] Davidson D W and Cole R H 1951 *J. Chem. Phys.* **19** 1417
Davidson D W 1961 *Can. J. Chem.* **39** 571
[5] Scher H and Lax M 1973 *Phys. Rev.* B **7** 4491
[6] Moynihan C T, Boesch L P and Laberge N L 1973 *Phys. Chem. Glasses* **14** 122
[7] Lindsey C P and Patterson G D 1980 *J. Chem. Phys.* **73** 3348
[8] Grassberger P and Procaccia I 1982 *J. Chem. Phys.* **77** 6281
[9] Niklasson G A 1989 *J. Appl. Phys.* **66** 4350
[10] Feldman Y, Kozlovich N and Alexandrov Y 1996 *Phys. Rev.* E **54** 5420
[11] Leòn C, Santamaria J, Paris M A, Sanz J, Ibarra J and Varez A 1998 *J. Non-Cryst. Solids* **235–237** 753
[12] Macdonald J R 2001 *Phys. Rev.* B **63** 205 052205
[13] Macdonald J R 2002 *J. Chem. Phys.* **116** 3401
[14] Macdonald J R 2003 *J. Chem. Phys.* **118** 3258
[15] Macdonald J R 2009 *J. Phys. Chem. Solids* **70** 546
[16] Nigmatullin R R and Ryabov Y E 1997 *Phys. Solid State* **39** 87
[17] Dyre J C and Schroder T B 2000 *Rev. Mod. Phys.* **72** 873
[18] Dyre J C, Maass P, Roling B and Sidebottom D L 2009 *Rep. Prog. Phys.* **72** 046501
[19] Macdonald J R 2009 *J. Phys. Chem.* B **113** 9179
[20] Sidebottom D L 2009 *Rev. Mod. Phys.* **81** 999
[21] Macdonald J R 2010 *J. Appl. Phys.* **107** 10101
[22] Puzenko A, Ben Ishai P and Feldman Y 2010 *Phys. Rev. Lett.* **105** 037601
[23] Chang H and Jaffe G 1952 *J. Chem. Phys.* **20** 1071
[24] Macdonald J R 1953 *Phys. Rev.* **92** 4
[25] Friauf R J 1954 *J. Chem. Phys.* **22** 1329
[26] Macdonald J R 1971 *J. Electroanal. Chem.* **32** 317
[27] Macdonald J R 1973 *J. Chem. Phys.* **58** 4982 correction
Macdonald J R 1974 *J. Chem. Phys.* **60** 343
[28] Macdonald J R and Franceschetti D R 1978 *J. Chem. Phys.* **68** 1614
[29] Macdonald J R and Franceschetti D R 1979 *J. Electronal. Chem.* **99** 283
[30] Macdonald J R and Potter L D Jr 1987 *Solid State Ion.* **23** 61
Macdonald J R 2000 *J. Comput. Phys.* **157** 280
[31] Macdonald J R 1988 *J. Electrochem. Soc.* **135** 2274
[32] Franceschetti D R, Macdonald J R and Buck R P 1991 *J. Electrochem. Soc.* **138** 1368
[33] Klein R J, Zhang S, Dou S, Jones B H, Colby R H and Runt J 2006 *J. Chem. Phys.* **124** 144903
[34] Macdonald J R, Evangelista L R, Lenzi E K and Barbero G 2011 *J. Phys. Chem.* C **115** 7648
[35] Macdonald J R 2011 *J. Phys. Chem.* A **115** 13370
[36] Evangelista L R, Lenzi E K, Barbero G and Macdonald J R 2011 *J. Phys.: Condens. Matter* **23** 485005
See also Santoro P A, de Paula J L, Lenzi E K and Evangelista L R 2011 *J. Chem. Phys.* **135** 114704
[37] Krohns S, Lunkenheimer P, Ebbinghaus S G and Loidl A 2007 *Appl. Phys. Lett.* **91** 022910
[38] Jadżyn J and Swiergiel J 2012 *Indust. Eng. Chem. Res.* **51** 807
[39] Lenzi E K, Fernandez P R G, Petrucci T, Mulai H and Ribeiro H V 2011 *Phys. Rev.* E **84** 041128
[40] Bodor S, Zook J M, Lindner E and Gyurcsányi R E 2008 *Analyst* **133** 635
[41] Barbero G 2011 *J. Chem. Phys.* **135** 234505
[42] Gelman A and Fung K 2012 *Am. Sci.* **100** 6
[43] Alexe-Ionescu A L, Barbero G and Lelidis I 2009 *Phys. Rev.* E **80** 061203